AIMS Materials Science

http://www.aimspress.com/journal/Materials/

AIMS Materials Science, 4(5): 1052-1061.
DOI: 10.3934/matersci.2017.5.1052
Received: 13 July 2017
Accepted: 17 September 2017
Published: 22 September 2017

Research article

Coherent spin dynamics in a helical arrangement of molecular dipoles

Elena Díaz [1], Rafael Gutiérrez [2], Christopher Gaul [1,3], Gianaurelio Cuniberti [2,4,5], and Francisco Domínguez-Adame [1,*]

[1] GISC, Departamento de Física de Materiales, Universidad Complutense, E-28040 Madrid, Spain
[2] Institute for Materials Science, Dresden University of Technology, 01062 Dresden, Germany
[3] Cognitec Systems GmbH, Großenhainer Str. 101, 01127 Dresden, Germany
[4] Dresden Center for Computational Materials Science (DCMS), TU Dresden, 01062 Dresden, Germany
[5] Center for Advancing Electronics Dresden, TU Dresden, 01062 Dresden, Germany

[*] **Correspondence:** Email: adame@ucm.es.

Abstract: Experiments on electron transport through helical molecules have demonstrated the appearance of high spin selectivity, in spite of the rather weak spin-orbit coupling in organic compounds. Theoretical models usually rely on different mechanisms to explain these experiments, such as large spin-orbit coupling, quantum dephasing, the role of metallic contacts, or the interplay between a helicity-induced spin-orbit coupling and a strong dipole electric field. In this work we consider the coherent electron dynamics in the electric field created by the helical arrangement of dipoles of the molecule backbone, giving rise to an effective spin-orbit coupling. We calculate the spin projection onto the helical axis as a figure of merit for the assessment of the spin dynamics in a very long helical molecule. We prove that the spin projection reaches a steady state regime after a short transient. We compare its asymptotic value for different initial conditions, aiming to better understand the origin of the spin selectivity found in experiments.

Keywords: spin polarized transport; helical molecules; spin sensitivity; nanoscale materials; spin-orbit coupling

1. Introduction

Exploiting the spin degree of freedom to transfer information or perform logic operations builds the basis of spintronics. Currently, the majority of existing spintronic devices are based on inorganic materials. However, using organic molecules in spintronics, though very challenging, would offer many advantages such as the possibility for chemically tuning the spin-dependent response as well as

their inexpensive synthesis in large amounts. For molecules lacking a magnetic response, we might not expect any strong spin-dependent properties. Surprisingly, it has been experimentally shown under a variety of conditions that double-stranded DNA oligomers, bacteriorhodopsin, oligopeptides, and helicene molecules can act as strong spin filters [1–10]. Since the only common feature of all these system is their helical symmetry, the hypothesis has been suggested—and meanwhile there is strong experimental evidence supporting it—that the observed spin selectivity is tightly related to the chirality of the probed molecules. These results can have profound implications not only for the design of novel organic or bio-inspired spintronic devices, but also shed a new light on electron transfer in biologically relevant molecules.

On the theoretical side, several approaches related to spin selective transport in helical systems have been proposed [11–19]. They are based both on tight-binding-like models as well as on continuum approaches. Their common denominator—an exception is Ref. [17]—is the assumption that a non-conventional spin-orbit coupling (SOC) in a helical system can lead to the blocking of one type of spin component. Although it has been shown in these different studies that spin selectivity is possible, there is still in our view a lack of a unifying microscopic picture allowing to connect the specific features of the electronic structure of helical molecules to model parameters.

In this study, we investigate the coherent dynamics of an electronic wave packet propagating in the electric field created by a helical arrangement of dipoles. This field induces an effective SOC that resembles the Rashba-type spin-orbit interaction in semiconductors. However, here the SOC mirrors the global helical symmetry of the system. The model is inspired by previous studies reported in Refs. [13, 15]. We compute the spin projection onto the helical axis and consider it as a figure of merit for the assessment of the spin dynamics in a long helical molecule. We prove that the spin projection reaches a steady state regime after a quick transient and compare its asymptotic value for different initial conditions, aiming at a better understanding of the origin of the spin selectivity found in experiments. It is worth mentioning that we focus on the coherent electron dynamics only and neglect dissipation hereafter. Nevertheless, dissipation may play a key role in experiments on electron transport through helical molecules and more realistic models need to consider its impact [14, 20–22].

2. Model Hamiltonian

Electric dipoles are common in the backbone of helical molecules, like the alpha helix. The backbone with a helical arrangement of peptides dipoles wraps the cylindrical structure of the molecule. Therefore, an electron moving along the axis of the helical molecule interacts with the electric field created by the dipoles. In the reference frame of the moving electron, the electric field induces a magnetic field, thus leading to a Rashba-like SOC.

We are concerned with a very long helix of radius R directed along the Z axis with axially oriented dipoles, as depicted in Figure 1. The point dipoles are labeled by an integer index n running from $-\infty$ to ∞. They are located at $\boldsymbol{r}_n = n\Delta z\,\hat{\boldsymbol{e}}_z + R\,\hat{\boldsymbol{\rho}}_n$ and their dipole moments are $\boldsymbol{d}_n = d\,\hat{\boldsymbol{e}}_z$. Δz is the spacing of the z component of the position vector of the dipoles and the pitch of the helix is $b = N_d\Delta z$, where N_d is the number of dipoles per turn. Here, we have used cylindrical coordinates so that $\hat{\boldsymbol{\rho}}_n = (\cos\varphi_n, \sin\varphi_n, 0)$ with $\varphi_n = 2\pi n/N_d + \pi$. The constant angle π added to φ_n is only introduced for convenience. It represents a π-rotation about the molecule axis that does not affect the physical magnitudes.

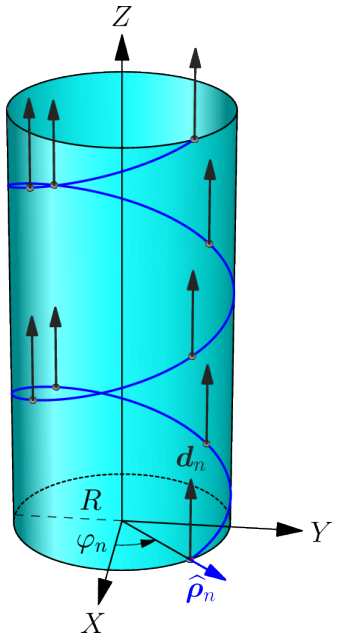

Figure 1. An electron in a given spin state is moving along the axis Z of a helical arrangement of electric dipoles $\boldsymbol{d}_n$. The electric field created by the dipoles induces a magnetic field in the rest frame of the electron and hence influences its spin dynamics.

Each dipole contributes to the total electric field of the molecule as follows [23]

$$\boldsymbol{E}(\boldsymbol{r}) = \frac{1}{4\pi\epsilon_0}\sum_{n=-\infty}^{\infty}\left[3\,\frac{(\boldsymbol{r}-\boldsymbol{r}_n)\cdot\boldsymbol{d}_n}{|\boldsymbol{r}-\boldsymbol{r}_n|^5}\,(\boldsymbol{r}-\boldsymbol{r}_n) - \frac{\boldsymbol{d}_n}{|\boldsymbol{r}-\boldsymbol{r}_n|^3}\right]. \tag{1}$$

Now we calculate the components of the electric field (1) in the XY plane for they are needed to obtain the SOC. Since the dipoles are parallel to the molecule axis, we get

$$\begin{aligned} E_x(\boldsymbol{r}) &= \frac{3d}{4\pi\epsilon_0}\sum_{n=-\infty}^{\infty}\frac{z-n\Delta z}{|\boldsymbol{r}-\boldsymbol{r}_n|^5}\,(x-x_n)\,, \\ E_y(\boldsymbol{r}) &= \frac{3d}{4\pi\epsilon_0}\sum_{n=-\infty}^{\infty}\frac{z-n\Delta z}{|\boldsymbol{r}-\boldsymbol{r}_n|^5}\,(y-y_n)\,. \end{aligned} \tag{2}$$

We will neglect the electron motion out of the molecular axis hereafter. In this case, the position vector is $\boldsymbol{r} = z\,\hat{\boldsymbol{e}}_z$ when the electron moves along the Z axis. Setting $x = y = 0$ in Eq. (2) yields

$$\begin{aligned} E_x(z) &= -\frac{3Rd}{4\pi\epsilon_0}\sum_{n=-\infty}^{\infty}\frac{(z-n\Delta z)\cos\varphi_n}{\left[R^2+(z-n\,\Delta z)^2\right]^{5/2}}\,, \\ E_y(z) &= -\frac{3Rd}{4\pi\epsilon_0}\sum_{n=-\infty}^{\infty}\frac{(z-n\Delta z)\sin\varphi_n}{\left[R^2+(z-n\,\Delta z)^2\right]^{5/2}}\,. \end{aligned} \tag{3}$$

For the calculation of the SOC, we will need to evaluate $\mathcal{E}(z) = -i\left[E_x(z) - iE_y(z)\right]$ (see Ref. [15] for further details). From Eq. (3) we obtain

$$\mathcal{E}(z) = -i\,\frac{3Rd}{4\pi\epsilon_0}\sum_{n=-\infty}^{\infty}\frac{(z-n\,\Delta z)\,e^{-i2\pi n/N_d}}{\left[R^2+(z-n\,\Delta z)^2\right]^{5/2}}\,. \tag{4}$$

For the typical values of the parameters found in helical molecules, it turns out that $\Delta z \ll b$, namely $N_d \gg 1$. Under this premise, we can replace the sum over n in Eq. (4) by an integral. To this end, we introduce the dimensionless variable $u = (z - n\Delta z)/b$ and make the formal substitution $\sum_n \to (b/\Delta z)\int du$ in the summation appearing in Eq. (4). Thus

$$\sum_{n=-\infty}^{\infty}\frac{(z-n\,\Delta z)\,e^{-i2\pi(z-n\Delta z)/b}}{\left[R^2+(z-n\,\Delta z)^2\right]^{5/2}} \simeq \frac{1}{b^3\Delta z}\int_{-\infty}^{\infty}du\,\frac{u\,e^{i2\pi u}}{(u^2+R^2/b^2)^{5/2}}\,. \tag{5}$$

After performing the integration we obtain

$$\mathcal{E}(z) = \frac{2\pi d}{\epsilon_0\Delta z b^2}\,K_1(2\pi R/b)\,e^{-i2\pi z/b} \equiv \mathcal{D}_0\,e^{-i2\pi z/b}\,, \tag{6}$$

where K_1 is the modified Bessel function of the second kind. Taking $R/b = 1/4$ as a typical value in helical molecules, then $K_1(2\pi R/b) \simeq 1/4$. It is worth mentioning that a similar result appears when the electric dipoles are contained in the XY plane but with a different constant $\mathcal{D}_0$. Therefore, the precise orientation of the dipoles do not affect qualitatively our conclusions.

The SOC Hamiltonian arises as a relativistic correction to the electron motion along the molecular axis Z [24]. Heuristically it can be understood as the result of the interaction between the electron spin and the magnetic field induced by the electric field $\boldsymbol{E}$ in the rest frame of the electron. The SOC Hamiltonian is expressed as $\hat{\mathcal{H}}_{\rm SO} = \lambda\boldsymbol{\sigma}\cdot(\hat{\boldsymbol{p}}\times\boldsymbol{E})$, symmetrized such that the Hamiltonian is Hermitian. Here $\lambda = e\hbar/(2mc)^2$ and $\boldsymbol{\sigma}$ is a vector whose components are the Pauli matrices σ_x, σ_y, and σ_z. For $\hat{\boldsymbol{p}} = \hat{p}\,\hat{\boldsymbol{e}}_z$ the SOC Hamiltonian reduces to

$$\hat{\mathcal{H}}_{\rm SO} = \frac{\lambda}{2}\left[\hat{p}_z\begin{pmatrix}0 & \mathcal{E}(z)\\ \mathcal{E}^*(z) & 0\end{pmatrix} + \begin{pmatrix}0 & \mathcal{E}(z)\\ \mathcal{E}^*(z) & 0\end{pmatrix}\hat{p}_z\right]. \tag{7}$$

The total Hamiltonian of the electron moving along the molecular axis subject to the SOC is $\hat{\mathcal{H}} = \hat{p}^2/2m + \hat{\mathcal{H}}_{\rm SO}$. The electrostatic potential due to the helical arrangement of dipoles is constant along the molecular axis and it can then be neglected. Taking Eq. (6) into account, the Hamiltonian can be cast in the form $\hat{\mathcal{H}} = E_b\hat{H}$ where the dimensionless Hamiltonian $\hat{H}$ reads

$$\hat{H} = -\frac{\partial^2}{\partial\xi^2} - 2\pi\gamma\begin{pmatrix}0 & e^{-i2\pi\xi}\left(i\,\dfrac{\partial}{\partial\xi}+\pi\right)\\ e^{i2\pi\xi}\left(i\,\dfrac{\partial}{\partial\xi}-\pi\right) & 0\end{pmatrix}. \tag{8}$$

For the sake of simplicity we have defined $E_b = \hbar^2/2mb^2$, $\xi = z/b$, and the dimensionless spin-orbit parameter $\gamma = \hbar\lambda\mathcal{D}_0/(2\pi bE_b)$. Previous models in the literature have estimated a phenomenological SOC to be of the order of $\hbar\lambda\mathcal{D}_0 = 4 - 12\,\text{meV nm}$ [13], what defines a reasonable range for our dimensionless SOC parameter as $\gamma = 0.06 - 0.2$.

3. Steady States in a Helical Molecule

The dimensionless Hamiltonian (8) is not translation invariant but it commutes with the helical operator $\hat{q} = \hat{p} + \pi\sigma_z$, which has the eigenstates

$$\boldsymbol{\chi}(\xi) = \begin{pmatrix} \chi_1 e^{i(q-\pi)\xi} \\ \chi_2 e^{i(q+\pi)\xi} \end{pmatrix} . \tag{9}$$

Inserting the ansatz (9) into the dimensionless Schrödinger equation $\hat{H}\chi(\xi) = \varepsilon\chi(\xi)$ yields the following eigenenergies

$$\varepsilon_{qs} = q^2 + \pi^2 - 2\pi s\sqrt{1+\gamma^2}\, q \equiv (q - q_s)^2 - \pi^2\gamma^2 , \qquad s = \pm 1 . \tag{10}$$

The energy as a function of the helical momentum splits into two parabolas (free electrons) displaced by an amount $q_s = s\pi\sqrt{1+\gamma^2}$ from the origin. Thus, the helical conformation of the electric dipoles brings in the additional effective momentum q_s. The additional momentum arising from the helical geometry of organic molecules can have an impact on the optical transitions as well [25].

The corresponding normalized eigenfunctions of the dimensionless Hamiltonian (8) are easily found to be

$$\boldsymbol{\chi}_{qs}(\xi) = \frac{1}{2}\begin{pmatrix} [(1+s)\cos\phi + (1-s)\sin\phi]e^{i(q-\pi)\xi} \\ [(1-s)\cos\phi - (1+s)\sin\phi]e^{i(q+\pi)\xi} \end{pmatrix} , \tag{11}$$

with

$$\tan\phi = \frac{\gamma}{1+\sqrt{1+\gamma^2}} . \tag{12}$$

4. Coherent Spin Dynamics

We turn to the problem we are interested in, namely the dynamics of an electron wave packet with a given spin state. To proceed, we expand any arbitrary solution to the time-dependent Schrödinger equation $i\partial_t\chi(\xi,t) = \hat{H}\chi(\xi,t)$ in terms of the eigenvectors of the Hamiltonian (8) as follows

$$\boldsymbol{\chi}(\xi,t) = \sum_s \int_{-\infty}^{\infty} \frac{dq}{2\pi} C_{qs}\boldsymbol{\chi}_{qs}(\xi)\, e^{-i\varepsilon_{qs}t} , \tag{13}$$

where time is expressed in units of $\hbar/E_b$ and

$$C_{qs} = \int_{-\infty}^{\infty} d\xi\, \boldsymbol{\chi}^{\dagger}_{qs}(\xi)\cdot\boldsymbol{\chi}(\xi,0) . \tag{14}$$

Consider an initial wave packet $f(\xi)$ of dimensionless width W given as

$$\boldsymbol{\chi}(\xi,0) = f(\xi)\left(\cos(\theta)\,\boldsymbol{u}_{\uparrow} + e^{i\varphi}\sin(\theta)\,\boldsymbol{u}_{\downarrow}\right) , \tag{15}$$

where $\boldsymbol{u}_\sigma$ with $\sigma = \uparrow, \downarrow$ denotes an eigenvector of σ_z. For the sake of concreteness we set $\varphi = 0$ hereafter. When $\theta = 0$ ($\theta = \pi/2$), the spin of the initial wave packet is parallel (antiparallel) to the

molecule axis and we will refer to as *fully polarized state*. Similarly, when $\theta = \pi/4$, the spin of the initial wave packet is directed along the X axis. We will name such state as *fully unpolarized* in the sense that the initial spin is out of the molecule axis.

Notice that we assume the same spatial function $f(\xi)$ for both components of the initial wave packet $\chi(\xi, 0)$. This is not a serious limitation but calculations are largely simplified. We take a Gaussian spatial function of the form

$$f(\xi) = \left(\frac{1}{2\pi W^2}\right)^{1/4} \exp\left(ik\xi - \frac{\xi^2}{4W^2}\right), \tag{16}$$

where k is the initial momentum and W is the standard deviation. A lengthy but straightforward calculation from Eq. (13) yields

$$\begin{aligned}\chi_\uparrow(\xi,t) = e^{-i\pi(\xi+\pi t)}\Big\{ &\cos\theta\, \cos^2\phi\, G_-(\xi+\omega t,t) + \cos\theta\, \sin^2\phi\, G_-(\xi-\omega t,t) \\ &- \frac{1}{2}\sin\theta\sin(2\phi)\left[G_+(\xi+\omega t,t) - G_+(\xi-\omega t,t)\right]\Big\}, \end{aligned} \tag{17}$$

$$\begin{aligned}\chi_\downarrow(\xi,t) = e^{i\pi(\xi-\pi t)}\Big\{ &\sin\theta\, \sin^2\phi\, G_+(\xi+\omega t,t) + \sin\theta\, \cos^2\phi\, G_+(\xi-\omega t,t) \\ &- \frac{1}{2}\cos\theta\sin(2\phi)\left[G_-(\xi+\omega t,t) - G_-(\xi-\omega t,t)\right]\Big\}, \end{aligned} \tag{18}$$

where $\omega = 2\pi\sqrt{1+\gamma^2}$ and

$$G_\pm(y,t) = \left(\frac{W^2}{2\pi}\right)^{1/4} \frac{1}{\sqrt{W^2+it}}\, \exp\left\{-\frac{y^2/4 + i(\pi \mp k)\left[(\pi \mp k)t \pm y\right]W^2}{W^2+it}\right\}. \tag{19}$$

As an example, Figure 2 depicts the short-time ($0 < t < 1$) behavior of $|\chi_\uparrow(\xi,t)|^2$ and $|\chi_\downarrow(\xi,t)|^2$ of an initially fully polarized ($\theta = 0$) Gaussian wave packet of width $W = 1$ and $k = 1$ when the dimensionless SOC is $\gamma = 0.2$. Although initially the lower component vanishes $\chi_\downarrow(\xi,0) = 0$ (hard to see in Figure 2), it grows very quickly but remains much smaller than the upper component $\chi_\uparrow(\xi,t)$. Therefore, the SOC leads to a partial depolarization of the initially fully polarized Gaussian wave packet.

5. Spin Projection

We now focus on the spin projection (SP) onto the direction of the electron momentum, i.e., along the molecule axis

$$\begin{aligned}\mathrm{SP}(t) = \int_{-\infty}^{\infty} d\xi\, \chi^\dagger(\xi,t)\sigma_z\chi(\xi,t) &= \cos(2\phi)\int_{-\infty}^{\infty}\frac{dq}{2\pi}\left[|C_{q,+1}|^2 - |C_{q,-1}|^2\right] \\ &+ 2\sin(2\phi)\int_{-\infty}^{\infty}\frac{dq}{2\pi}\,\mathrm{Re}\left[C^*_{q,+1}C_{q,-1}e^{i(\varepsilon_{q,+1}-\varepsilon_{q,-1})t}\right]. \end{aligned} \tag{20}$$

This magnitude, also known as helicity, becomes time-dependent because the operator σ_z does not commute with the Hamiltonian (8). In other words, the spin projection onto the direction of the electron momentum is not conserved. Nevertheless, we will show that the last term in Eq. (20) vanishes after a quick transient and SP(t) reaches an asymptotic value as time evolves.

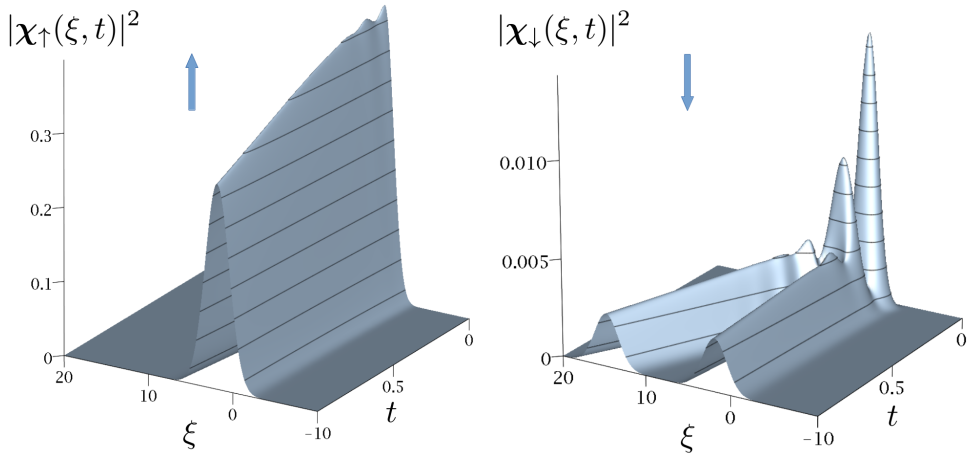

Figure 2. Short-time dynamics of an initially fully polarized ($\theta = 0$) Gaussian wave packet of width $W = 1$ and $k = 1$ when the dimensionless SOC is $\gamma = 0.2$. Notice the different vertical scale for the upper and lower components.

Let us consider an initially fully polarized ($\theta = 0$ or $\theta = \pi/2$) Gaussian wave packet as that shown in Figure 2. We can calculate SP(t) from Eq. (20) to obtain

$$\mathrm{SP}(t) = \pm\cos^2(2\phi) + \mathrm{Re}\left[e^{\mp i2\omega\pi t}\int_{-\infty}^{\infty} d\xi\, f^*(\xi)f(\xi+2\omega t)\right]\sin^2(2\phi)\,. \tag{21}$$

The upper and lower sign refers to spin up ($\theta = 0$) and down ($\theta = \pi/2$), respectively. After a straightforward calculation, one obtains a closed expression for SP(t) that has a transient contribution which vanishes at large times $t \gg W/\omega$. A transient time $W/\omega \sim 40\,\mathrm{fs}$ is roughly estimated for a highly localized initial state with $W = 1$ passing through a helical molecule with a SOC parameter of $\gamma = 0.1$. Thus, after a quick transient regime, the spin projection reaches the asymptotic value given as $\mathrm{SP}_\infty = \mathrm{SP}(t \to \infty)$ with

$$\mathrm{SP}_\infty = \pm\cos^2(2\phi) = \pm\frac{1}{1+\gamma^2}\,. \tag{22}$$

Therefore, the larger the SOC parameter, the smaller the asymptotic spin projection. The result above mentioned is not surprising. An initial wave packet with a well defined spin projection such that $|\mathrm{SP}(0)| = 1$ get their components mixed as time evolves because of the presence of the SOC. At long time, the spin projection diminishes and finally $|\mathrm{SP}_\infty| < 1$.

The dynamics of a wave packet with vanishing initial spin projection is more interesting because it becomes spin polarized along the molecule axis after being transmitted through the molecule. Therefore, we now consider a fully unpolarized initial wave packet with $\theta = \pi/4$. From Eq. (21) we find that the asymptotic spin projection is non zero, given as

$$\mathrm{SP}_\infty = -\frac{\gamma}{1+\gamma^2}\int_{-\infty}^{\infty} d\xi\,|f(\xi)|^2\cos(2\pi\xi) = -\frac{\gamma}{1+\gamma^2}\,e^{-2\pi^2W^2}\,. \tag{23}$$

For a narrow initial wave packet ($W \ll 1$), the integral in Eq. (23) becomes unity and then $\mathrm{SP}_\infty \simeq -\gamma/(1+\gamma^2)$. In this case $|\mathrm{SP}(0)| = 0$ but the spin projection becomes nonzero with time and reaches a finite value such that $|\mathrm{SP}_\infty| \neq 0$.

Figure 3 depicts the absolute value of the asymptotic spin projection as a function of the dimensionless SOC parameter γ for initially polarized ($\theta = 0$) and fully unpolarized ($\theta = \pi/4$) wave packets. In the former case, $|SP_\infty|$ monotonously decreases on increasing γ, as expected. However, the behavior of $|SP_\infty|$ for an initially fully unpolarized wave packet is more complex. At low values of γ the asymptotic $|SP_\infty|$ increases upon increasing the SOC and reaches a maximum value of 50% at $\gamma = 1$. On the contrary, a further increase of γ above unity yields smaller $|SP_\infty|$.

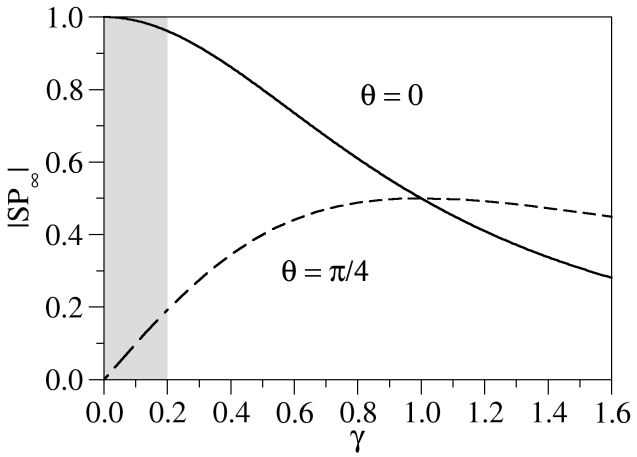

Figure 3. Absolute value of the asymptotic spin projection as a function of the dimensionless SOC parameter for initially polarized ($\theta = 0$) and fully unpolarized ($\theta = \pi/4$) wave packets. The gray area highlights the region with realistic values of γ according to our estimations.

Finally, let us discuss how the particular chirality of the molecule would affect our main results. The chirality in our model is directly related to the sign of the magnitude b, the pitch of the helix. If $b > 0$ ($b < 0$) we will be dealing with a right (left)-handed helix. In addition, the SOC parameter γ is inversely proportional to b, so the chirality of the molecule will define a particular sign of γ. Therefore, chirality will not affect the asymptotic SP_∞ of an initial state which is fully polarized [see Eq. (22)]. Remarkably, for the most interesting situation, namely the polarization of an initially unpolarized state, SP_∞ is completely reversed, as a clear signature related to the molecular chirality [see Eq. (23)].

6. Conclusion

In summary, we have considered the coherent spin dynamics of electrons subject to the electric field created by a helical arrangement of dipoles. The electric field induces a Rashba-like SOC of electrons moving along the helical axis. This coupling can be understood as the result of the interaction between the electron spin and the magnetic field induced by the electric field in the rest frame of the electron. Once the model was presented, we were able to solve it exactly and to obtain a closed expression for the electron wave packet. We also calculated the spin projection onto the helical axis as a figure of merit to assess the spin dynamics in the molecular system. Remarkably, we found that the spin projection reaches a steady state regime after a quick transient. We then obtained the asymptotic value for a fully spin-polarized initial wave packet and concluded that the electron becomes partially depolarized as time evolves. Similarly, an initially unpolarized wave packet gets partially polarized

along the molecule axis due to the SOC induced by the helical arrangement of dipoles.

Acknowledgments

Work in Madrid was supported by the Spanish MINECO under Grants MAT2013-46308 and MAT2016-75955. RG and GC acknowledge financial support from the Volkswagen Stiftung via grant No. 88366 (Spintronic Components based on Chiral Molecules). This work has also been partly supported by the German Research Foundation (DFG) within the Cluster of Excellence "Center for Advancing Electronics Dresden". We acknowledge the Center for Information Services and High Performance Computing (ZIH) at TU Dresden for computational resources.

Conflict of Interest

The authors declare that there is no conflict of interest regarding the publication of this manuscript.

References

1. Göhler B, Hamelbeck V, Markus TZ, et al. (2011) Spin selectivity in electron transmission through self-assembled monolayers of double-stranded DNA. *Science* 331: 894–897.
2. Xie Z, Markus TZ, Cohen SR, et al. (2011) Spin specific electron conduction through DNA oligomers. *Nano Lett* 11: 4652–4655.
3. Mishra D, Markus TZ, Naaman R, et al. (2013) Spin-dependent electron transmission through bacteriorhodopsin embedded in purple membrane. *Proc Nat Acad Sci USA* 110: 14872–14876.
4. Kettner M, Gohler B, Zacharias H, et al. (2015) Spin filtering in electron transport through chiral oligopeptides. *J Phys Chem C* 119: 14542–14547.
5. Mondal PC, Fontanesi C, Waldeck DH, et al. (2015) Field and chirality effects on electrochemical charge transfer rates: Spin dependent electrochemistry. *ACS Nano* 9: 3377–3384.
6. Rosenberg RA, Mishra D, Naaman R (2015) Chiral selective chemistry induced by natural selection of spin-polarized electrons. *Angew Chem Int Edit* 54: 7295–7298.
7. Einati H, Mishra D, Friedman N, et al. (2015) Light-controlled spin filtering in bacteriorhodopsin. *Nano Lett* 15: 1052–1056.
8. Ben Dor O, Yochelis S, Mathew SP, et al. (2013) A Chiral-based magnetic memory device without a permanent magnet. *Nat Commun* 4: 2256.
9. Michaeli K, Varade V, Naaman R, et al. (2017) A new approach towards spintronics—Spintronics with no magnets. *J Phys-Condens Mat* 29: 103002.
10. Kiran V, Mathew SP, Cohen SR, et al. (2016) Helicenes—A new class of organic spin filter. *Adv Mater* 28: 1957–1962.
11. Yeganeh S, Ratner MA, Medina E, et al. (2009) Chiral electron transport: Scattering through helical potentials. *J Chem Phys* 131: 014707.
12. Medina E, Lopez F, Ratner M, et al. (2012) Chiral molecular films as electron polarizers and polarization modulators. *EPL* 99: 17006.

13. Gutiérrez R, Díaz E, Naaman R, et al. (2012) Spin-selective transport through helical molecular systems. *Phys Rev B* 85: 081404.

14. Guo AM, Sun QF (2012) Spin-selective transport of electrons in DNA double helix. *Phys Rev Lett* 108: 218102.

15. Gutierrez R, Díaz E, Gaul C, et al. (2013) Modeling Spin transport in helical fields: Derivation of an effective low-dimensional Hamiltonian. *J Phys Chem C* 117: 22276–22284.

16. Vager D, Vager Z (2012) Spin order without magnetism: A new phase of spontaneously broken symmetry in condensed matter. *Phys Lett A* 376: 1895–1897.

17. Gersten J, Kaasbjerg K, Nitzan A (2013) Induced spin filtering in electron transmission through chiral molecular layers adsorbed on metals with strong spin-orbit coupling. *J Chem Phys* 139: 114111–114130.

18. Guo AM, Díaz E, Gaul C, et al. (2014) Contact effects in spin transport along double-helical molecules. *Phys Rev B* 89: 205434.

19. Matityahu S, Utsumi Y, Aharony A, et al. (2016) Spin-dependent transport through a chiral molecule in the presence of spin-orbit interaction and nonunitary effects. *Phys Rev B* 93: 075407.

20. Guo AM, Sun QF (2012) Sequence-dependent spin-selective tunneling along double-stranded DNA. *Phys Rev B* 86: 115441.

21. Guo AM, Sun QF (2014) Spin-dependent electron transport in protein-like single-helical molecules. *Proc Natl Acad Sci USA* 111: 11658.

22. Pan TR, Guo AM, Sun QF (2016) Spin-polarized electron transport through helicene molecular junctions. *Phys Rev B* 94: 235448.

23. Jackson JD (1999) *Classical Electrodynamics*, Third Edition, New York: Wiley, 146.

24. Greiner W (2000) *Relativistic Quantum Mechanics*, Berlin: Springer.

25. Díaz E, Malyshev AV, Domínguez-Adame F (2007) Interband optical transitions in DNA-like systems. *Phys Rev B* 76: 205117.

AIMS Press